BIOCHEMISTRY
including biophysical chemistry & molecular biology

Article

pubs.acs.org/biochemistry

The Monomeric Species of the Regulatory Domain of Tyrosine Hydroxylase Has a Low Conformational Stability

José L. Neira,*[,†,‡] Felipe Hornos,[†] Julio Bacarizo,[§,∥] Ana Cámara-Artigás,[§] and Javier Gómez[†]

[†]Instituto de Biología Molecular y Celular, Universidad Miguel Hernández, 03202 Elche (Alicante), Spain

[‡]Biocomputation and Complex Systems Physics Institute, 50009 Zaragoza, Spain

[§]Department of Physical Chemistry, Biochemistry and Inorganic Chemistry, University of Almería, Agrifood Campus of International Excellence (ceiA3), Almería, Spain

Supporting Information

ABSTRACT: Tyrosine hydroxylase (TyrH) catalyzes the hydroxylation of tyrosine to form 3,4-dihydroxyphenylalanine, the first step in the synthesis of catecholamine neurotransmitters. The protein contains a 159-residue regulatory domain (RD) at its N-terminus that forms dimers in solution; the N-terminal region of RDTyrH (residues 1−71) is absent in the solution structure of the domain. We have characterized the conformational stability of two species of RDTyrH (one containing the N-terminal region and another lacking the first 64 residues) to clarify how that N-terminal region modulates the conformational stability of RD. Under the conditions used in this study, the RD species lacking the first 64 residues is a monomer at pH 7.0, with a small conformational stability at 25 °C (4.7 ± 0.8 kcal mol^{-1}). On the other hand, the entire RDTyrH is dimeric at physiological pH, with an estimated dissociation constant of 1.6 μM, as determined by zonal gel filtration chromatography; dimer dissociation was spectroscopically silent to circular dichroism but not to fluoresecence. Both RD species were disordered below physiological pH, but the acquisition of secondary native-like structure occurs at pHs lower than those measured for the attainment of tertiary native- and compactness-like arrangements.

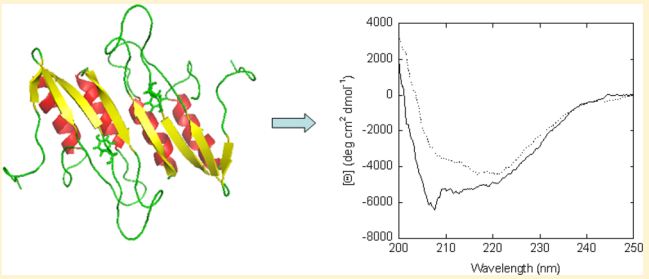

Tyrosine hydroxylase (TyrH) is the enzyme that catalyzes the rate-limiting step in catecholamine biosynthesis.[1,2] It catalyzes the conversion of tyrosine to 3,4-dihydroxyphenylalanine, which is the precursor for the neurotransmitters norepinephrine, epinephrine, and dopamine. Dysregulation of TyrH is associated with bipolar disorder, schizophrenia, and hypertension due to the key role played by those neurotransmitters in the autonomous nervous system.[3−6] TyrH belongs to the family of pterin-dependent aromatic amino acid hydroxylases, together with phenylalanine hydroxylase (PheH) and tryptophan hydroxylase.[7] By using O_2 and BH_4 as the other substrates, together with the related amino acid, the three enzymes catalyze the hydroxylation of their corresponding residue.[7]

Rat TyrH is a 498-residue polypeptide chain,[8] which forms tetramers through its C-terminus.[9] Each monomer is composed of an N-terminal RD (containing ∼160−200 amino acids, depending on the species), a catalytic domain (∼300 residues), and a C-terminal tetramerization domain (∼45 amino acids).[10,11] The NMR solution structure of the RD of TyrH, RDTyrH, shows a largely unfolded N-terminal region (residues 1−71) and a well-folded C-terminal portion (residues 72−159). The C-terminal region, as concluded from the solution structure of the truncated version of the RD containing residues 65−159,[12] is formed by a four-stranded antiparallel β-sheet (β1, residues 75−77; β2, residues 80−84; β3, residues 110−116; and β4, residues 131−137) and two α-helices (α1, residues 97−106; and α2, residues 139−152) connected by five loops; the helices are parallel with and on one side of the sheet[12] (Figure 1). This structure is very similar to the crystal structure of the RD of PheH.[13] The isolated RDTyrRH in solution is a homodimer, forming an ACT domain dimer[14] composed of an eight-stranded β-sheet with four helices on one side of the sheet; the dimerization interface is composed of strand β3 and helix α1, burying a small surface area (770 Å^2 for each monomer, which is ∼12% of the total monomer surface area).

In this report, we describe the conformational stabilities of two variants of RDTyrH. With the first one, lacking residues 1−64 ($RDTyrH_{65-159}$), we attempted to study the conformational stability and structure, at different pHs, of the isolated well-folded region of RDTyrH. With the second species, containing the 64 disordered residues at the N-terminus (RDTyrH), we attempted to evaluate the influence, if any, of those residues on the conformational stability and structure of the protein. Our results suggest that the stability of the well-folded region of the RD is very small (4.7 ± 0.8 kcal mol^{-1}, at 25 °C and pH 7.0). The N-terminal residues seem to affect the stability of the RD through the solvent exposure of the accessible surface area (ASA).

Received: February 14, 2016
Revised: May 4, 2016
Published: May 25, 2016

DOI: 10.1021/acs.biochem.6b00135
Biochemistry 2016, 55, 3418−3431

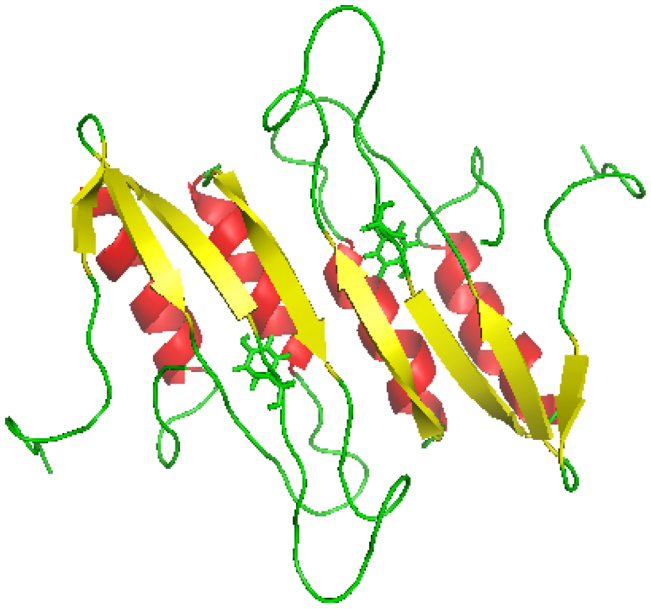

Figure 1. Structure of $RDTyrH_{65-159}$. The dimeric solution structure of the domain is shown with the elements of secondary structure in different colors (Protein Data Bank entry 2MDA): β-strands in yellow and α-helices in red. The sole Tyr131 is shown as sticks. This figure was produced with Pymol.[55]

Thermally induced denaturations of both proteins were shown to be irreversible at both pH 4.0 and 7.5, precluding the determination of the thermodynamic parameters of the unfolding reaction, because it is under kinetic control. Both proteins were populating partially folded species at pH <7.0, with apparent flexible secondary structure and a lack of tertiary structure, which may involve self-associated molecules. The acquisition of secondary native-like structure occurs at pHs lower than those measured for the attainment of tertiary native- and compactness-like scaffolds, populating molten-globule-like species. The RDTyrH species dimerized with a K_D of 1.6 μM, but the self-association process was spectroscopically silent by CD.

EXPERIMENTAL PROCEDURES

Materials. Ultrapure urea and GdmCl were from ICN Biomedicals Inc. Their concentrations were calculated as described previously.[15] Trizma acid and base, NaCl, the sodium dodecyl sulfate (SDS) low-molecular weight protein markers (containing bovine serum albumin, ovalbumin from chicken egg, glyceraldehyde-3-phosphatase dehydrogenase from rabbit muscle, carbonic anhydrase from bovine erythrocytes, trypsinogen from bovine pancreas, trypsin inhibitor from soybean, α-lactalbumin from bovine milk, and aprotinin from bovine lung), ultrapure dioxane, and ANS were from Sigma. The low-molecular weight marker for the gel filtration column (containing ribonuclease A, chymotrypsinogen A, ovalbumin, albumin, and blue dextran 2000) was from GE Healthcare (Barcelona, Spain). Dialysis tubing with a molecular weight cutoff of 3500 Da was from Spectrapore. Standard suppliers were used for all other chemicals. Water was deionized and purified on a Millipore system.

Protein Expression and Purification. The vectors of both proteins were a kind gift from P. F. Fitzpatrick (The University of Texas Health Science Center at San Antonio, San Antonio, TX). The expressions and purifications of RDTyrH and $RDTyrH_{65-159}$ were conducted as described previously.[12] The only variation in the protocol was the substitution of the mixture of inhibitors (1 μM leupeptin, 1 μM pepstatin, and 250 μg/mL phenylmethanesulfonyl fluoride) with a tablet of Sigma protease cocktail during the lysis step. The purities of all protein preparations used were >95% based on SDS–polyacrylamide gel electrophoresis.

NMR Spectroscopy. The NMR experiments were conducted at 20 °C on a Bruker Avance DRX-500 spectrometer equipped with a triple-resonance probe and z-pulsed field gradients.

One-Dimensional (1D) NMR Experiments. Homonuclear 1D NMR experiments were performed with RDTyrH and $RDTyrH_{65-159}$ at a concentration of 150 μM (in protomer units) in 0.5 mL, (i) at pH 7.0 in 50 mM phosphate buffer or (ii) at pH 4.5 (50 mM deuterated acetic acid) in H_2O/D_2O buffer [90%/10% (v/v)] (uncorrected for deuterium isotope effects). TSP was used as the external chemical shift reference. The 1D ^1H spectra were acquired with 16K data points, with 512 scans and a 6000 Hz spectral width (12 ppm), by using the WATERGATE sequence.[16] Baseline correction and zero filling were applied before processing. All spectra were processed and analyzed by using TopSpin 2.1 (Bruker GmbH, Karlsruhe, Germany) working on a personal computer.

Translational Diffusion Measurements (DOSY experiments). These were performed with the pulsed-gradient spin–echo sequence, by using the same procedures described elsewhere.[17,18] Further experimental details are provided in the Supporting Information.

Size Exclusion Chromatography (SEC). This technique was used to determine the R_S values of RDTyrH and $RDTyrH_{65-159}$.[19−21] Protein concentrations ranged from 50 to 750 μM. Experiments were performed at 20 °C. Samples were loaded in 50 mM phosphate buffer (pH 7.0), 150 mM NaCl (to avoid interactions with the column), and 2 mM EDTA (to avoid protein degradation) in a calibrated Superdex 75 10/30 HR FPLC column (GE Healthcare). In all chromatograms, the elution volumes were obtained from analyses with UNICORN software (GE Healthcare). The void volume (7.54 ± 0.06 mL) was determined from blue dextran and the bed volume (18.98 ± 0.03 mL) from conductivity measurements. Samples were eluted at a rate of 1 mL/min and continuously monitored with an online detector at a wavelength of 280 nm.

As the elution volume of RDTyrH was dependent on protein concentration (see Results), the pH and urea denaturation experiments were conducted at a protein concentration of 100 μM (in protomer units). For $RDTyrH_{65-159}$, a protein concentration of 100 μM (in protomer units) was also used. For the pH denaturation experiments, the corresponding buffer (see below) was prepared at a final concentration of 50 mM, containing 150 mM NaCl and 2 mM EDTA. Urea denaturation experiments were conducted at pH 7.0 (50 mM phosphate buffer) with 150 mM NaCl and 2 mM EDTA.

The standards used in column calibration and their corresponding R_S values were as follows: ribonuclease A (16.4 Å), chymotrypsinogen (20.9 Å), ovalbumin (30.5 Å), and bovine serum albumin (35.5 Å).[22] Elution volumes of these were acquired only under native conditions: pH 7.0 (50 mM phosphate buffer) with 150 mM NaCl. Protein concentrations for the standards were in the range of 10–20 μM.

The weight-average partition coefficients (σ) of protein standards and RD species were calculated with the equation $\sigma = (V_e - V_o)/V_i$. The σ values were transformed by using the inverse error function complement $[\mathrm{erfc}^{-1}(\sigma)]$, which yields[21,22]

DOI: 10.1021/acs.biochem.6b00135
Biochemistry 2016, 55, 3418–3431

$$R_S = a + b[\mathrm{erf}\, c^{-1}(\sigma)] \quad (1)$$

where a and b are constants. The inverse error function complement is[23] $\sigma = 1 - (2/\sqrt{\pi}) \int_0^u e^{-x^2} dx$, and the function under the integral is the Gaussian function of probability.

Fluorescence. Spectra were recorded at 25 °C on a Cary Varian spectrofluorimeter (Agilent), with a Peltier temperature controller. Sample concentrations were 20 μM (in protomer units) in the pH and chemical denaturation experiments for both RD species, and also 30 μM (in protomer units) for RDTyrH. The final concentrations of the buffers were, in all cases, 10 mM. The experiments were set up the day before and left overnight at 5 °C. Control experiments were also conducted after a 2 h incubation at room temperature; no differences with those prepared the day before were observed. A 1 cm path length quartz cell (Hellma) was used.

Intrinsic Fluorescence. Protein samples were excited at 278 nm in the pH range from 2.0 to 12.0. The rest of the experimental parameters has been described elsewhere.[17,24] Appropriate blank corrections were added to all spectra.

Chemical denaturations at pH 7.0 (phosphate buffer), followed by fluorescence or CD, were conducted by dilution of the proper amount of an 8 M urea stock solution. Fluorescence experiments were also performed in GdmCl (from a 7 M stock solution). All the denaturations in urea were shown to be reversible by following $\langle\lambda\rangle$ (see below) for both proteins at a concentration of 20 μM (in protomer units) (Figure 1 of the Supporting Information).

The pH of each sample was measured after completion of pH denaturations with an ultrathin Aldrich electrode in a Radiometer (Copenhagen, Denmark) pH-meter. The salts and acids used have been described elsewhere.[17,20,24] The reversibility of the pH denaturations was tested by using 1D ^{1}H NMR experiments. Experiments were conducted at physiological pH for each protein, and then the corresponding RD species was exchanged at pH 4.5 by using Amicon centrifugal devices; spectra were recorded at that pH, then the proteins exchanged back at physiological pH by using Amicon centrifugal devices, and new spectra recorded and compared with those obtained previously. In both proteins, the spectra recorded were identical (data not shown).

The wavelength-averaged emission intensity (also called the spectrum mass center), $\langle\lambda\rangle$, was calculated as described previously.[17,25] Briefly, the wavelength-averaged emission intensity, $\langle\lambda\rangle$, is $\langle\lambda\rangle = \frac{\sum_1^n \frac{1}{\lambda_i} I_i}{\sum_1^n I_i}$, where I_i is the intensity at wavelength λ_i. From its definition, the parameter is an integral of the value of the fluorescence spectrum, and thus, it allows us to obtain information over all the intensities acquired in the spectrum (instead of using a single one, which is usually done when following denaturations in fluorescence). We report $\langle\lambda\rangle$ in units of μm^{-1}. Chemical and pH denaturations were repeated three times with new samples at any of the concentrations assayed.

Thermal Denaturations. These were performed at constant heating rates of 60 °C/h and an average time of 1 s. The "average time" is the "sampling time" of the instrument at each temperature. Ideally, in a thermal scan experiment, this time should be much lower than the scan rate of the experiment, to ensure that the temperature is constant during the acquisition of fluorescence emission at a particular temperature [under our conditions, the temperature change during the sampling time (0.017 °C) was negligible]. Thermal scans were conducted at 308 nm by excitation at 278 nm from 25 to 85 (or 95) °C. The rest of the experimental set was the same as described above. The thermal denaturations for both species were not reversible at any pH.

Fluorescence Quenching. Quenching by either iodide or acrylamide was examined under different solution conditions. Protein concentrations were 20 μM (in protomer units). Excitation was at 278 nm; emission was measured from 300 to 400 nm. In the quenching with KI, the ionic strength was kept constant by addition of KCl; also, $Na_2S_2O_3$ was added to a final concentration of 0.1 M to prevent formation of I_3^-. The presence of KCl did not modify the structure of RDTyrH or $RDTyrH_{65-159}$, based on the absence of changes in the shape and ellipticity of the CD spectra in the presence of KCl (0−1 M) (data not shown). The slit width was set at 5 nm for both excitation and emission. For quenching with KI, the data were fitted to[26]

$$F_0/F = 1 + K_{sv}[X] \quad (2)$$

where K_{sv} is the Stern−Volmer constant for collisional quenching, F_0 is the fluorescence when no KI is present, and F is the fluorescence at any KI concentration. The range of KI concentrations explored was 0−0.7 M. We explored the quenching at pH 4.0 (acetate buffer) and pH 7.0 (Tris buffer). Experiments were also conducted in the presence of 6 M urea at pH 7.0 (10 mM Tris buffer).

For acrylamide quenching, the experimental parameters were the same as with KI. However, the Stern−Volmer equation was modified to include an exponential term to account for dynamic quenching [$F_0/F = (1 + K_{sv}[X])e^{\nu[X]}$,[26] where ν is the dynamic quenching constant]. This equation is identical to eq 2 when ν = 0.

ANS Binding. The excitation wavelength was 380 nm, and emission was measured from 400 to 600 nm. Slit widths were 5 nm for excitation and emission lights. ANS stock solutions were prepared in water and diluted to yield a final concentration of 100 μM. Blank solutions were subtracted from the corresponding spectra. ANS was used to monitor the pH denaturation of both proteins and the urea denaturation of $RDTyrH_{65-159}$ [at 20 μM protein (in protomer units)]. In the pH denaturation experiments, protein concentrations were 15 μM (in protomer units).

Circular Dichroism (CD). Circular dichroism spectra were recorded on a Jasco J810 (Japan) spectropolarimeter fitted with a thermostated cell holder and interfaced with a Peltier unit. The instrument was periodically calibrated with (+)-10-camphorsulfonic acid. Molar ellipticity was calculated as described previously.[21]

Far-UV Spectra. Isothermal wavelength spectra of RDTyrH and $RDTyrH_{65-159}$ at different pHs or urea concentrations were recorded at a scan speed of 50 nm/min with a response time of 4 s and averaged over six scans at 25 °C, in a 0.1 cm path length cell. Protein concentrations ranged from 20 to 50 μM for each protein (in protomer units) in 10 mM buffer. Spectra were corrected by subtracting the baseline in all cases. The chemical and pH denaturations were repeated at least three times with new samples. The samples were prepared the day before and left overnight at 5 °C to allow for equilibration.

Thermal Denaturation Experiments. The experiments were performed at constant heating rates of 60 °C/h and a response time of 8 s. Thermal scans were collected in the far-UV region following the changes in ellipticity at 222 nm from 25 to 80 °C in 0.1 cm path length cells with a total protein concentration of 20

DOI: 10.1021/acs.biochem.6b00135
Biochemistry 2016, 55, 3418−3431

Table 1. Hydrodynamic Measurements for Both RD Species

	$RDTyrH_{65-159}$		RDTyrH	
technique	conditions	property measured[a]	conditions	property measured[a]
DOSY NMR	43 μM, pH 7.0, 50 mM phosphate buffer, 20 °C	$(8.4 \pm 0.5) \times 10^{-7}$ $cm^2\ s^{-1}$ (16 ± 2 Å)	150 μM, pH 7.0, 50 mM phosphate buffer, 20 °C	$(5.42 \pm 0.05) \times 10^{-7}$ $cm^2\ s^{-1}$ (26 ± 2 Å)
	330 μM, pH 7.0, 50 mM phosphate buffer, 20 °C	$(7.93 \pm 0.07) \times 10^{-7}$ $cm^2\ s^{-1}$ (16 ± 2 Å)	150 μM, pH 4.5, 50 mM acetate buffer, 20 °C	$(4.38 \pm 0.07) \times 10^{-7}$ $cm^2\ s^{-1}$
	60 μM, pH 4.5, 50 mM acetate buffer, 20 °C	$(7.4 \pm 0.3) \times 10^{-7}$ $cm^2\ s^{-1}$		
DLS[b]	277 μM, pH 7.5, 50 mM Hepes buffer, 20 °C	2.7 ± 0.2 nm (12.5 kDa)	554 μM, pH 7.5, 100 mM Hepes buffer, 20 °C	4.8 ± 0.7 nm (34.7 kDa)
	277 μM, pH 4.0, 50 mM acetate buffer, 20 °C	3.7 ± 0.8 nm (21.8 kDa)	554 μM, pH 4.0, 100 mM acetate buffer, 20 °C	7 ± 1 nm (80.9 kDa)
	554 μM, pH 7.5, 50 mM Hepes buffer, 20 °C	2.6 ± 0.3 nm (12.1 kDa)		
	554 μM, pH 4.0, 50 mM acetate buffer, 20 °C	3.6 ± 0.3 nm (21.7 kDa)		
	800 μM, pH 7.5, 50 mM Hepes buffer, 20 °C	2.4 ± 0.9 nm (12.0 kDa)		
	800 μM, pH 4.0, 50 mM acetate buffer, 20 °C	4.5 ± 0.6 nm (35.0 kDa)		
SEC[c]	70 μM, pH 7.0, 50 mM Tris buffer with 150 mM NaCl and 2 mM EDTA, 20 °C	12.14 ± 0.06 mL	58 μM, pH 7.0, 50 mM Tris buffer with 150 mM NaCl and 2 mM EDTA, 20 °C	9.76 ± 0.08 mL
	140 μM, pH 7.5, 100 mM Tris buffer with 150 mM NaCl and 2 mM EDTA, 20 °C	12.07 ± 0.04	230 μM, pH 7.0, 50 mM Tris buffer with 150 mM NaCl and 2 mM EDTA, 20 °C	9.67 ± 0.02 mL
	277 μM, pH 7.0, 50 mM Tris buffer with 150 mM NaCl and 2 mM EDTA, 20 °C	12.11 ± 0.08	600 μM, pH 7.0, 50 mM Tris buffer with 150 mM NaCl and 2 mM EDTA, 20 °C	9.66 ± 0.03
	540 μM, pH 7.0, 50 mM Tris buffer with 150 mM NaCl and 2 mM EDTA, 20 °C	12.10 ± 0.05		

[a]In the DOSY experiments, the magnitude measured is the translational diffusion coefficient, D (in parentheses, the R_S is indicated at the physiological pHs), in DLS measurements R_S, and in SEC experiments the elution volume, given as the average of three measurements. [b]In each measurement, the calculated molecular weight assuming a spherical shape is given within parentheses. [c]The calculated R_S was 21 ± 2 Å at all elution volumes in $RDTyrH_{65-159}$. The calculated R_S for RDTyrH at the highest concentrations was 34 ± 2 Å. Not all the concentrations explored for RDTyrH are included (see Figure 2C).

μM (in protomer units). Solution conditions were the same as those reported in the steady-state experiments. No difference was observed between the scans aimed to test drifting of the spectropolarimeter. Thermal denaturations were not reversible at any pH for any RD protein, as shown by (i) the comparison of spectra before and after heating and (ii) the changes in the voltage of the instrument.[27]

Dynamic Light Scattering (DLS). DLS measurements were performed with a Zetasizer Nano ZS (Malvern Instruments Ltd.) using a thermostated 12 μL quartz sample cuvette. Samples of protein were prepared at different concentrations [280, 577, and 800 μM (in protomer units)] in 50 mM acetate buffer (pH 4.0) and in 50 mM Hepes buffer (pH 7.0). All the solutions were filtered; immediately before measurements, protein samples were centrifuged for 30 min at 14000 rpm and room temperature to remove any aggregates and dust. Measurements were performed on each sample at 20 °C to determine the R_S. Data were analyzed using the software developed by Malvern Instruments Ltd. The R_S and molecular weight were determined from the Stokes−Einstein equation, assuming a spherical shape for both proteins.

It is important to stress here that we used a 50 mM phosphate buffer concentration in SEC, ITC (see below), NMR, and DLS measurements, whereas we used a final buffer concentration of 10 mM in the CD and fluorescence experiments. We used a higher concentration of buffer in SEC, ITC (see below), NMR, and DLS experiments because of the higher protein concentration (in protomer units) used. When preparing the quenching experiments, we did not observe any change in the shape of the far-UV CD spectrum of both proteins when the control experiments were conducted at 0 and 1 M KCl.

Analysis of the pH, Thermal, and Chemical Denaturation Curves, and Free Energy Determination. The pH denaturations were analyzed assuming that both protein species, protonated and deprotonated, contributed to the spectral properties:

$$X = \frac{X_a + X_b 10^{n(pH - pK_a)}}{1 + 10^{n(pH - pK_a)}} \quad (3)$$

where X is the spectral property being observed (ellipticity, fluorescence intensity, or $\langle\lambda\rangle$), X_a is that for the acidic species, X_b is that observed at high pHs, pK_a is the apparent midpoint of the titrating group, and n is the Hill coefficient (which was close to 1 in all the curves reported in this work). The apparent pK_a reported (from intrinsic or ANS fluorescence and CD) was obtained from three different measurements in each technique, prepared with new samples.

The thermal and chemical denaturation data for monomeric species were fitted to the two-state equation

$$X = (X_N + X_D e^{-\Delta G/RT})/(1 + e^{-\Delta G/RT}) \quad (4)$$

where R is the gas constant, ΔG is the denaturation free energy, and T is the temperature in kelvin. X_N and X_D correspond to the physical property of the native and denatured protein, respectively, being monitored. Both parameters showed a linear relationship with the temperature or the denaturant concentration.

Chemical denaturation curves for $RDTyrH_{65-159}$ were analyzed according to the linear extrapolation model, in which the free energy is given by $\Delta G = m([D]_{1/2} - [D])$,[15] where [D] is the denaturant concentration, $[D]_{1/2}$ is that at the midpoint of the transition, and m is the slope of the curve.

The equations given above must be modified (by the introduction of a concentration-dependent term)[28−30] if dissociation of a self-associated species is explored. Because in our measurements of $RDTyrH_{65-159}$, no dissociation of dimeric species was observed [as we did not observe a protein concentration dependence in the spectroscopic signals (see

DOI: 10.1021/acs.biochem.6b00135
Biochemistry 2016, 55, 3418−3431

Results)], we used the equations given above without any concentration-dependent term. However, we did observe a concentration dependence in the fluorescence signal of RDTyrH and then in a dimeric equilibrium (see Results). The thermal and chemical denaturation data for a dimeric species were fitted to the two-state equation:[29,30]

$$X = X_N - (X_N - X_D)e^{-\Delta G/RT}\left[\frac{\left(1 + \frac{8C_t}{e^{-\Delta G/RT}}\right)^{1/2} - 1}{4C_t}\right] \quad (5)$$

where the ΔG in chemical denaturations would be given by the equation $\Delta G = m([D]_{1/2} - [D]) - RT\ln(C_t)$, where C_t is the total protein monomer concentration.

It is important to indicate here that the use in fluorescence of $\langle\lambda\rangle$ (an intensive variable)[30] or the emission intensity (an extensive variable) at 308 nm yielded the same chemical denaturation thermodynamic parameters for both proteins, and both will be used in Results.

Fitting by nonlinear least-squares analysis to eqs 4 and 5 was performed by using Kaleidagraph (Abelbeck software) working on a personal computer.

Isothermal Titration Calorimetry (ITC). The ITC experiments were conducted by using a VP-ITC instrument (MicroCal, Northampton, MA). Before the calorimetric experiments, the proteins were concentrated and dialyzed at 4 °C against 50 mM Tris and 400 mM NaCl (pH 7.5). Dilution ITC experiments involved sequential injections of microliter amounts (20 μL) of a stock of concentrated protein (ranging from 300 to 700 μM (in protomer units)) into the calorimetric cell (1.4 mL); the cell initially contained isolated buffer.

Differential Scanning Calorimetry (DSC). DSC experiments were performed with a VP-DSC calorimeter (MicroCal). Protein solutions were prepared by exhaustive dialysis against 50 mM Tris and 400 mM NaCl (pH 7.5) at 5 °C. Experiments were conducted and results processed as previously described.[17] Further experimental details are provided in the Supporting Information.

RESULTS

RDTyrH$_{65-159}$ Is a Monomeric Species at Physiological pH and Low Concentrations. To map the hydrodynamic properties of both species, we used three complementary hydrodynamic techniques: SEC, DLS, and DOSY NMR measurements. Furthermore, we tried to measure the self-association reaction of both proteins by ITC. All the reported values were obtained at 20 °C.

RDTyrH$_{65-159}$. The DOSY NMR measurements provide the translational diffusion coefficient (D) at the concentrations used (Table 1). The values are similar, within error: the smaller error at the highest concentration was due to the better signal-to-noise ratio of the spectra, because it is unlikely that at 43 μM the fragment showed a stronger tendency to aggregate than at 330 μM. The average value from both measurements was $(8.2 \pm 0.5) \times 10^{-7}$ cm^2 s^{-1}. By taking into account the R_S of dioxane, and its D under our conditions $[(6.8 \pm 0.2) \times 10^{-6}$ cm^2 s$^{-1}]$, we obtained an R_S for the protein of 16 ± 2 Å.

The DLS measurements were taken at three concentrations: 277 μM (Figure 2A), 554 μM (Figure 2A of the Supporting Information) and 800 μM (Figure 2B of the Supporting Information) (all concentrations in protomer units); the

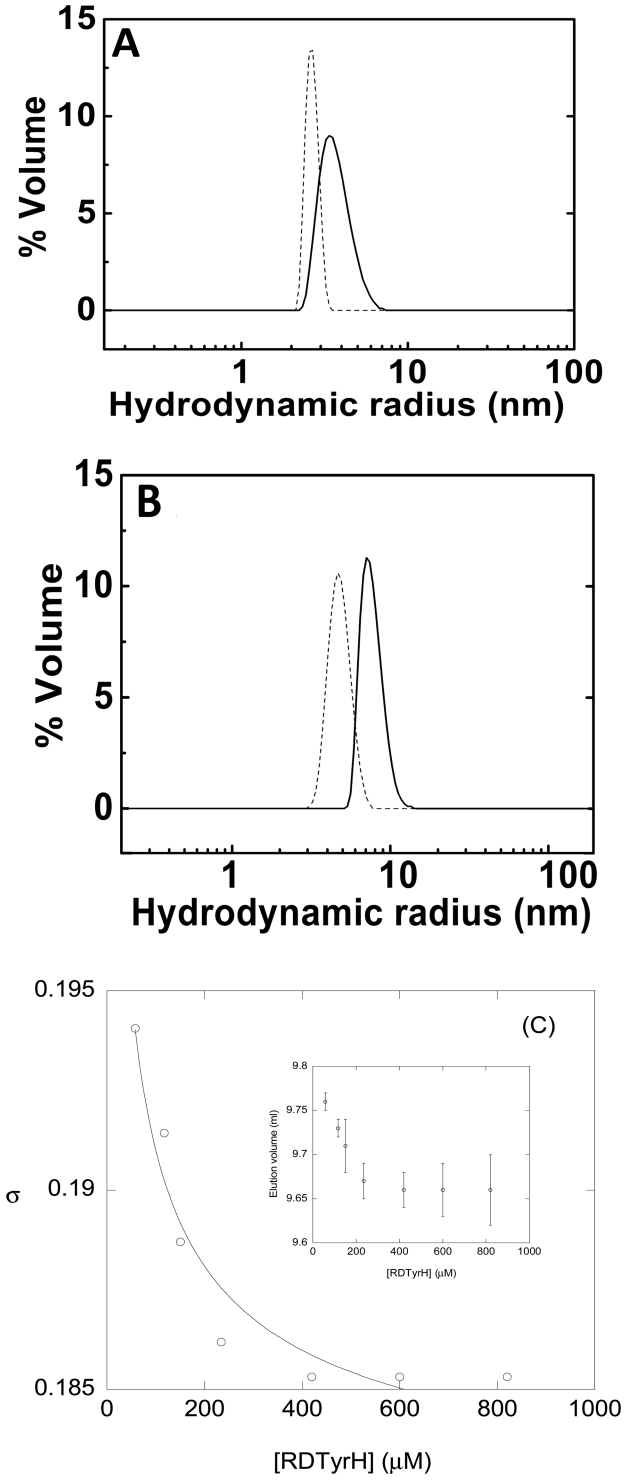

Figure 2. Hydrodynamic measurements of RDTyrH species. (A) DLS of RDTyrH$_{65-159}$ at 277 μM at pH 7.0 (---) and pH 4.5 (—). (B) DLS of RDTyrH at 277 μM (monomer concentration) at pH 7.0 (---) and pH 4.5 (—). (C) Changes in σ as the concentration of monomeric RDTyrH was increased. The fitting values were $\sigma_m = 0.50 \pm 0.09$ (the fitting was largely independent of this parameter, and thus, it was not properly determined) and $\sigma_d = 0.18 \pm 0.01$. The inset shows changes in elution volume (milliliters) as the concentration of monomeric RDTyrH was increased (the error bars are from at least three independent volume measurements for each protein concentration). Conditions were as follows: 20 °C, in Tris buffer (pH 7.0), 50 mM, with 150 mM NaCl and 2 mM EDTA.

DOI: 10.1021/acs.biochem.6b00135
Biochemistry 2016, 55, 3418−3431

obtained R_S values were virtually the same at the three concentrations (26 ± 3), and the estimated molecular weight was 12 kDa, assuming a spherical shape (by using the Stokes–Einstein equation). However, it must be kept in mind that the DLS peak was somewhat broad (Figure 2A), and this broadness increased at 800 μM (Figure 2 of the Supporting Information), suggesting, probably, the presence of self-associated species at this high concentration (as observed in the dimeric NMR solution structure[12]). A measurement of this broadness is given by the polydispersity of the peak: 9.4% at 277 μM, 11% at 554 μM, and 24% at 800 μM.

SEC measurements in the concentration range of 70–540 μM yielded elution volumes of 12.14 ± 0.06 mL (the average of three measurements) to 12.07 ± 0.04 mL (Table 1 and Figure 3 of the Supporting Information); therefore, we can conclude that in this concentration range, the oligomerization state of the protein does not change. The calculated R_S from these data was 21 ± 2 Å.[20,22,23] It is important to note that if we use the proposed linear relationship between the molecular weight and σ of the protein,[31] then the apparent molecular weight should be similar to that of chymotrypsin (eluting at 12.33 ± 0.06 mL) (second arrow from the right in Figure 3A of the Supporting Information). We did not use this relationship, instead of that between R_S and σ (see Experimental Procedures), because in our column (Superdex 75 HR10, GE Healthcare) the linear relationship with the molecular weight and σ is worse than that with R_S (regression coefficient of 0.95 vs 0.99).

We also tried to see if the protein dissociated upon dilution using the heat evolved in the reaction as a probe monitored by ITC. No significant heat evolved upon dilution of the concentrated protein solution (ranging from 300 to 700 μM) into the calorimetric cell containing buffer (Figure 4 of the Supporting Information). These data suggest that either no self-association was happening or its dissociation constant is well below the minimal concentration of the diluted protein used in the calorimetric cell (the oligomeric form of the protein being the major fraction both in the syringe and in the cell). On the basis of the experimental (DLS, DOSY, and SEC results) and theoretical evidence (see the next paragraph), we favor the first explanation.

We can further elaborate on the expected theoretical value of the R_S for a protein of the size of RDTyrH$_{65-159}$. The R_S value for an ideal unsolvated spherical molecule can be theoretically calculated by considering that the anhydrous molecular volume, $M\bar{V}/N$, equals the volume of a sphere[31,32] of radius R: $R = \sqrt[3]{3M\bar{V}/4N\pi}$, where M is the molecular mass of the protein, $\bar{V}$ is its partial specific volume, and N is Avogadro's number. The molecular mass of monomeric RDTyrH$_{65-159}$ is 10470.8 Da, and $\bar{V}$ = 0.72 cm^3/g as calculated from the amino acid composition.[32] Then, the calculated R_S is 14.4 Å, but because the hydration shell is 3.2 Å wide,[33] the hydration radius would be around 17.6 Å, which is similar to that obtained from DOSY spectra (16 ± 2 Å) and smaller than that from DLS. In addition, it has been shown that the R_S of a folded spherical protein can be approximated by the relationship[18] $R_S = (4.75 \pm 1.11)N^{0.29}$, where N is the number of residues of the protein. In a 95-residue RDTyrH$_{65-159}$, this expression yields a value of 18 ± 4 Å, also similar to that determined by DOSY spectra. Finally, it is interesting to calculate the expected theoretical correlation time, τ_c, of the molecule, from the experimental measurements of D, according to the equation[34] $\tau_c = {}^2/_9(R_h^{ref}D^{ref})^2/D^3$ (where D_{ref} is the measured D for the dioxane and R_h^{ref} is its R_S) and to compare that figure with the one determined experimentally[12] for dimeric RDTyrH$_{65-159}$ (11.90 ± 0.02 ns). The calculated τ_c from the experimentally determined D was 9.02 ns, smaller, as could be expected, than that corresponding to the dimeric protein. Moreover, for a protein, the theoretically predicted τ_c is given by the equation $\tau_c = (9.18 \times 10^{-3}/T)\exp(2416/T)N^{0.93}$;[35] in a 95-residue protein, this yields a value 8.5 ns at 20 °C, and for a 190-residue protein, this number is 15.7 ns at the same temperature.

In summary, the three hydrodynamic techniques and the ITC data suggest that under our conditions, RDTyrH$_{65-159}$ remained basically monomeric, probably with an elongated shape.

RDTyrH. At a concentration of 150 μM, the D was (5.42 ± 0.05) × 10^{-7} cm^2 s^{-1}, which was, as expected (because of the larger number of residues), smaller than that of RDTyrH$_{65-159}$. This yields an R_S of 26 ± 2 Å (Table 1).

The DLS measurements yielded an R_S of 48 ± 7 Å, which resulted in an estimated molecular weight of 34.7 kDa for a spherical molecule, twice the molecular weight of RDTyrH (17043.74 Da) (Figure 2B). The peak was also broader (larger polydispersity) than that observed for the shorter species (Figure 2A). These results suggest that the dominant species of RDTyrH is dimeric, and they support the use of the monomer–dimer equilibrium in the gel filtration calculations (see below).

The SEC experiments showed a sigmoidal-like variation in elution volume from 9.76 mL (at 58 μM) to 9.66 mL (to 800 μM) (Figure 2C, inset); we could not explore lower concentrations because of the poor absorbance of the protein (because it contains only a single Tyr). The fairly constant elution volume at the higher concentrations yields an R_S of 34 ± 2 Å (Figure 3B of the Supporting Information), further supporting the idea that the protein under these conditions is not a monomer. Interestingly enough, some of the chromatograms also showed the presence of a minor peak at the void volume (7.54 ± 0.06 mL), suggesting the presence of aggregated species (Figure 3B of the Supporting Information). These results are in disagreement with what we observed in RDTyrH$_{65-159}$, where no species were present at the void volume of the column (Figure 3A of the Supporting Information).

We attempted to fit the sigmoidal-like behavior of the elution volume of RDTyrH (Figure 2C, inset) to the Ackers' equations[19,21,22] assuming a monomer–dimer equilibrium:

$$\sigma = \sigma_m\left[\frac{-1 + \sqrt{1 + 8(1/K_D)C_t}}{4(1/K_D)C_t}\right] + \sigma_d\left[1 - \frac{-1 + \sqrt{1 + 8(1/K_D)C_t}}{4(1/K_D)C_t}\right] \quad (6)$$

where σ_m and σ_d are the weight-average partition coefficients of the monomer and dimer, respectively, C_t is the concentration of RDTyrH (in monomer units), and K_D is the dissociation constant for the equilibrium RDTyrH$_2$ ↔ RDTyrH + RDTyrH. From eq 6, we obtained a K_D value of 1.6 μM; the σ_d was 0.18, and the σ_m was 0.61, the latter with a large uncertainty. It is important to keep in mind the uncertainties in σ_m and K_D, because they were obtained from a long extrapolation (Figure 2C, inset). Thus, we shall assume that the K_D is a low limit of the dissociation constant, but it is important to note that the small value of K_D supports previous analytical ultracentrifugation data where at RDTyrH concentrations of 5 μM, a dimeric population was observed.[12]

For this species, we also tried to see if the protein dissociated upon dilution, using the heat evolved in the reaction monitored

DOI: 10.1021/acs.biochem.6b00135
Biochemistry 2016, 55, 3418–3431

by ITC as a probe. For experiments performed at both 390 and 570 μM, the heat released upon dilution of the protein into the calorimetric cell was very small and consistent with a dissociation reaction only for the first injections when the concentration in the calorimetric cell was in the low micromolar range (Figure 4 of the Supporting Information). The amount of heat released for the first two injections (while the concentration in the cell remained below 10 μM) may reflect the dissociation of the dimeric species that rapidly tends to the normal dilution level as the total concentration in the cell exceeds the level. Unfortunately, because of the sensitivity limitations of the technique, we were unable to perform ITC experiments using a more diluted protein solution in the syringe. These results may be consistent with the dilution of a dimeric species with a dissociation constant in the low micromolar range (1−2 μM). Under these conditions, the dimerization equilibrium is effectively displaced only when the final protein concentration (in the cell) is very low (<10 μM) and the population of the dimer remains virtually unaffected when its initial concentration in the syringe (390−540 μM) changes to reach concentrations well above the value of its dissociation constant, K_D.

Both RD Species Acquired a Native-like Structure in a Narrow pH Range. If we want to measure the conformational stability of RDTyrH and the importance of the disordered tail, we must first determine in which pH range the proteins acquired a native-like structure. To that end, we used several spectroscopic and biophysical probes, namely, intrinsic fluorescence, ANS fluorescence, CD, NMR, DLS, and SEC. The whole set of techniques gives complementary information about different structural features of the polypeptide chain. We used intrinsic fluorescence to monitor changes in the tertiary structure of the protein, around its single tyrosine residue (Figure 1). We used ANS fluorescence to monitor the burial of solvent-exposed hydrophobic patches (and to detect the presence of possible partially folded species[36]). We conducted far-UV CD experiments to monitor the changes in secondary structure. We used NMR to elucidate whether there was evidence of residual structure at selected pHs and to measure their corresponding R_S values. We used DLS at pH 4.5 to determine the size of the species present (and, thus, to support the NMR results). Finally, we used SEC to determine the compactness.

Fluorescence. *Steady-State Fluorescence and Thermal Denaturations.* The fluorescence spectra of both species showed a maximum at 308 nm, due to the single Tyr131. The spectrum of RDTyrH has been reported previously,[11] and it is identical to that of the truncated version. $\langle\lambda\rangle$ [Figure 3A (●)] and the fluorescence intensity at 308 nm (data not shown) of $RDTyrH_{65-159}$ showed two transitions. The first occurred with a pK_a of 5.8 ± 0.3, and the second at basic pHs, probably because of the titration of the phenolic group of tyrosine; in this transition, no basic baseline was observed. On the other hand, RDTyrH also showed the same two titrations with a pK_a of 5.9 ± 0.2 for the first one similar to that of the shorter species [Figure 3A (○)].

Thermal denaturations at several pHs (4.5, 7.0, and 8.6) were conducted by following the changes in the intrinsic fluorescence of $RDTyrH_{65-159}$. At pH ≥7.0, we observed an irreversible sigmoidal behavior. Thermal denaturations followed by the fluorescence of RDTyrH at the same pHs also showed an irreversible sigmoidal behavior at pH >6.8.

ANS Binding. At low pH, the ANS fluorescence intensity at 480 nm was larger for both RD species and decreased as the pH was increased (Figure 3B), suggesting that at low pHs both

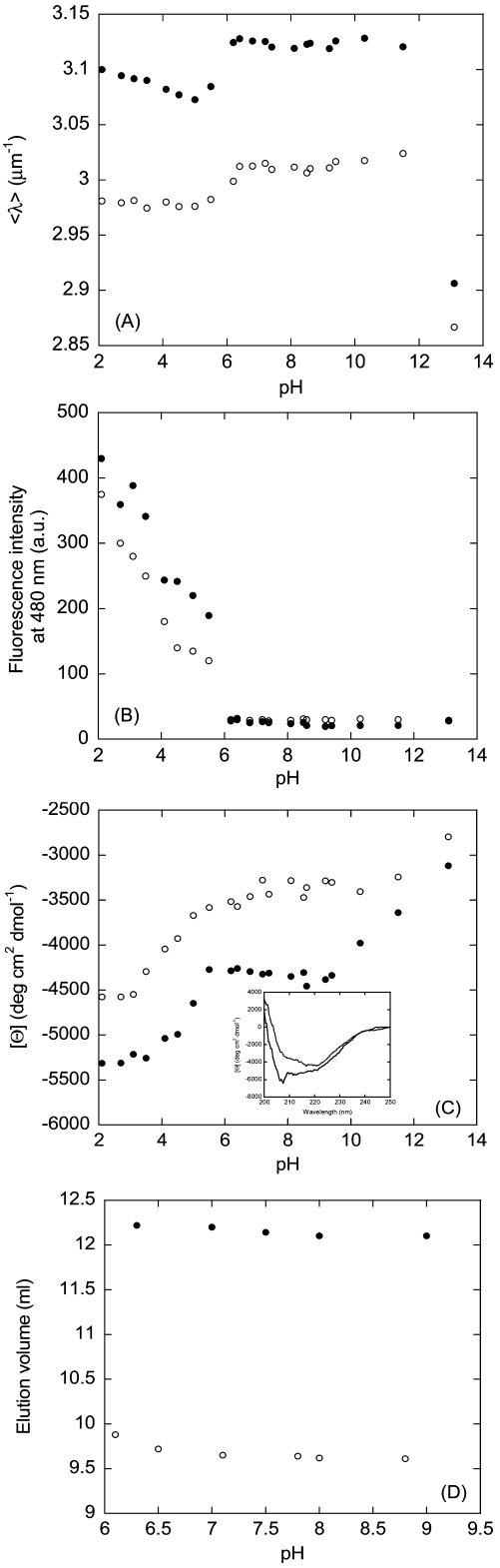

Figure 3. pH-induced structural changes in the RD species followed by spectroscopic and hydrodynamic techniques. (A) Changes in RD species [RDTyrH (○) and $RDTyrH_{65-159}$ (●)] in aqueous solution monitored by the changes in $\langle\lambda\rangle$ of the intrinsic fluorescence. (B) Changes in the intensity of ANS binding followed at 480 nm for both proteins (the same symbols that were used in panel A). The protein concentration was 15 μM (monomeric protein); ANS concentration was 100 μM, and the buffer concentration was 10 mM in all cases. (C) Changes in molar ellipticity at 222 nm, from far-UV spectra of both proteins (the same symbols that were used in panels A and B). The inset

DOI: 10.1021/acs.biochem.6b00135
Biochemistry 2016, 55, 3418−3431

Figure 3. continued

shows far-UV CD spectra of RDTyrH$_{65-159}$ at pH 4.5 (—) and pH 7.0 (---). Spectra were acquired in either 1 cm (fluorescence) or 0.1 cm (CD) path length cells. (D) Changes in elution volume (milliliters) as the pH was varied. At pH <6.0, the protein eluted at volumes larger than the bed volume (18.98 mL) of the column, and these data are not represented. Symbols for both proteins are as in panels A–C.

proteins had solvent-exposed hydrophobic regions. The intensity at 480 nm showed a sigmoidal-like behavior, but we could not determine its pK_a because of the absence of an acidic baseline. On the other hand, the $\langle\lambda\rangle$ of the fluorescence spectra of both proteins showed a pK_a of 5.4 ± 0.3 (data not shown), which is similar, within the error, to that determined by intrinsic fluorescence (Figure 3A).

Examination of Tyrosine Exposure by Fluorescence Quenching. To further examine the tertiary structure around Tyr131 and its solvent exposure, we studied iodide and acrylamide quenching in the presence and absence of denaturants (Table 2). In general, the K_{sv} parameters were identical for both proteins, suggesting that the environment around the sole Tyr131 was not modified by the presence of the N-terminal region. The values were also similar at any of the explored pHs, suggesting that the solvent accessibility of Tyr131 was similar. Furthermore, the K_{sv} values at physiological and low pHs were larger in acrylamide than in KI, as observed in other proteins.[20,24] The K_{sv} increased in the presence of urea at physiological pH when compared to that under physiological conditions in the absence of denaturant (Table 2). Taken together, these results indicate that Tyr131 was solvent-exposed (as suggested from the structure[12]) but not fully accessible at physiological pH.

Circular Dichroism. We took measurements only in the far-UV region, because the near-UV CD spectra of both species was lacking as previously reported,[11] because of the small amount of aromatic residues and the absence of an asymmetric environment for most of them.

The CD spectrum of RDTyrH at pH 7.0 has been described previously,[11] with minima at 208 and 222 nm, suggesting the presence of α-helical conformations. The CD spectrum of RDTyrH$_{65-159}$ (Figure 3C, inset) shows the same general shape at any pH as that of RD spectra, but with a slightly more intense minimum at 217 nm, suggesting the presence of a higher percentage of β-sheet (because of the removal of the N-terminal region). The shape of the spectra for both proteins did not change substantially as the pH was varied, but the spectra were more intense (in absolute value) at acidic pHs in both proteins. These results suggest that the proteins had more structure at those lower pHs (Figure 3C, inset), when there are some solvent-exposed hydrophobic patches, as shown by ANS experiments (Figure 3B). The change in ellipticity with pH followed a sigmoidal change with a pK_a of 4.75 ± 0.09 for RDTyrH$_{65-159}$ and 4.5 ± 0.2 for RDTyrH (Figure 3C); these values are smaller than those measured by fluorescence.

We also performed thermal denaturations at the same pHs used in fluorescence (4.5, 7.0, and 8.6) with RDTyrH$_{65-159}$. At pH ≥7.0, we observed sigmoidal behavior but the transitions were irreversible at any of the concentrations explored [from 15 to 50 μM protein (in protomer units)]. We also took DSC measurements of RDTyrH$_{65-159}$ at pH 7.5, and the denaturations were always strongly irreversible (data not shown), causing massive precipitation.

Thermal denaturations followed by CD in RDTyrH at the same pHs as the other species were also irreversible. We also took DSC measurements at pH 7.5, and the denaturations were always strongly irreversible (data not shown), causing massive precipitation. Because the thermal denaturations were always irreversible, we cannot further elaborate on the thermal stability of both proteins.

SEC Experiments. For both RDs, at pH <6.0, the protein did elute from the column at volumes larger than the bed volume (18.98 mL) (Figure 3D). These results suggest that both proteins, even though NaCl was present, were bound to the column at those pHs. We know from the experiments with ANS that at low pHs the proteins were partially folded (see above), with solvent-exposed hydrophobic patches. We hypothesize that those partially unfolded, solvent-exposed, and highly hydrophobic regions can interact with the column, resulting in larger elution volumes from the column (Figure 3B). At pH 6.0–7.0, the elution volume decreased until a constant volume (9.68 mL for RDTyrH and 12.26 mL for RDTyrH$_{65-159}$) was reached. Therefore, the protein did not get a native-like compactness until physiological pH had been reached.

NMR Experiments. As expected from its well-folded structure,[12] the 1D ^{1}H NMR spectra of both RD species at pH 7.0 had a large dispersion of signals in the aromatic and methyl regions (Figure 4 and Figure 5 of the Supporting Information). On the other hand, the 1D ^{1}H NMR spectra of RDTyrH$_{65-159}$ and RDTyrH at pH 4.5 did not show chemical shift dispersion in the amide and the aromatic regions or in the methyl regions (Figure 4A). We chose this pH because it is well inside the region in which the proteins had not acquired a native-like conformation, as concluded from the fluorescence and CD experiments (Figure 3). All the resonances were clustered together as expected for random-coil proteins,[37] namely, between 7.8 and 8.5 ppm (for the amide signals), between 6.8 and 7.5 ppm (for the aromatic signals) (Figure 4), and between 0.8 and 1.1 ppm (for the methyl protons) (Figure 5 of the Supporting Information). These results indicate that there was

Table 2. Quenching Parameters of Both RD Species in KI and Acrylamide[a]

	RDTyrH$_{65-159}$		RDTyrH	
conditions	K_{sv} (M^{-1}) (KI)	K_{sv} (M^{-1}) (acrylamide)[b]	K_{sv} (M^{-1}) (KI)	K_{sv} (M^{-1}) (acrylamide)[b]
pH 4.0	0.42 ± 0.04	4.2 ± 0.6 (1.89 ± 0.09)	0.38 ± 0.04	4.0 ± 0.3 (1.91 ± 0.09)
pH 7.0	0.26 ± 0.04	3.6 ± 0.4 (1.91 ± 0.09)	0.31 ± 0.04	3.9 ± 0.4 (1.91 ± 0.09)
6 M urea	1.43 ± 0.01	3.6 ± 0.1 (0)[c]	1.4 ± 0.1	3.6 ± 0.1 (0)[c]

[a]Errors are from fitting to eq 2. The K_{sv} values were obtained by fitting of fluorescence intensity at 315 nm vs the quenching agent concentration. Experiments were conducted at 25 °C. [b]The value within the parentheses is the ν, the dynamic quenching constant. [c]Acrylamide quenching in 6 M urea resulted in a straight line with a K_{sv} of 3.6 ± 0.1 M^{-1} in both proteins. The quenching experiments in the presence of urea were conducted at pH 7.0 in 10 mM Tris buffer.

DOI: 10.1021/acs.biochem.6b00135
Biochemistry 2016, 55, 3418–3431

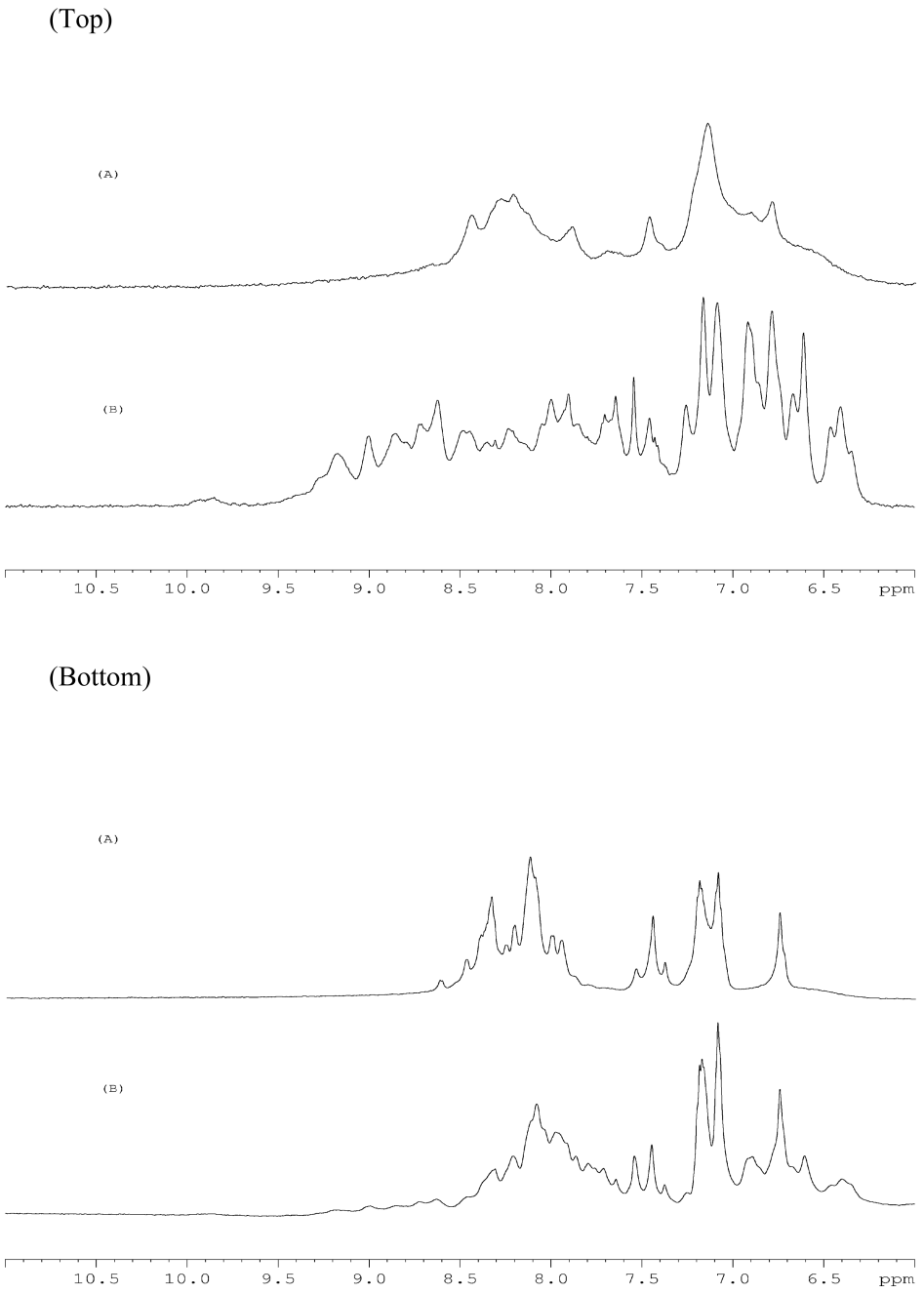

Figure 4. 1D ^{1}H NMR spectra of the RD species. (Top) Amide regions of RDTyrH$_{65-159}$ at (A) pH 4.5 and (B) pH 7.0 (B). (Bottom) Amide regions of RDTyrH at (A) pH 4.5 and (B) pH 7.0. Experiments were conducted at 20 °C with protein concentrations for both species of 150 μM (in protomer units).

no stable tertiary structure in any of the RD species at the low pH, but we cannot rule out the presence of nonstable, local secondary structure, as suggested by the higher intensity (in absolute value) at 222 nm in CD experiments (Figure 3C, inset).

We also performed DOSY measurements at pH 4.5 for both species. For RDTyrH, the D was $(4.38 \pm 0.07) \times 10^{-7}$ cm^2 s^{-1}, which was smaller than that measured at physiological pH [$(5.42 \pm 0.05) \times 10^{-7}$ cm^2 s^{-1}]. On the other hand, the D of RDTyrH$_{65-159}$ was $(7.4 \pm 0.3) \times 10^{-7}$ cm^2 s^{-1}, which was slightly smaller than that measured at pH 7.0 [$(8.2 \pm 0.5) \times 10^{-7}$ cm^2 s^{-1}]. These results suggest that both proteins were larger at acidic pH than at physiological pH: this larger size could be due to the presence of oligomeric species or, alternatively, to elongated (partially folded) populations.

DLS Experiments. At pH 4.5, the RDTyrH$_{65-159}$ had an R_S of 37 ± 8 Å, larger than the value measured at pH 7.0 (26 ± 2 Å), and the peak had a larger polydispersity [Figure 2A (—)]; this result yields an estimated molecular weight of 21.8 kDa for a spherical species. We observed a similar behavior at the two other protein concentrations of RDTyrH$_{65-159}$ assayed (554 and 800 μM) (Table 1 and Figure 2 of the Supporting Information). Therefore, the protein could be aggregated (forming a dimer), or alternatively, the protein could have an elongated shape. The expected theoretical R_S for a 95-residue unfolded protein[18] [$R_S = (2.21 \pm 1.07)N^{0.57\pm0.02}$] is 29 ± 2 Å, within the error of the value determined by DLS; however, the R_S for a well-folded [$R_S = (4.75 \pm 1.11)N^{0.29}$] tetrameric protein of that polypeptide length was 27 ± 2 Å, also similar to that value. Because the 1D ^{1}H NMR

DOI: 10.1021/acs.biochem.6b00135
Biochemistry 2016, 55, 3418−3431

Table 3. Thermodynamic Parameters of the RDTyrH Species Unfolding Reaction Obtained by Chemical Denaturation Experiments[a]

	$RDTyrH_{65-159}$				RDTyrH[e]			
biophysical probe	concentration (μM)	$\Delta G°$ (kcal mol^{-1})	m (kcal mol^{-1} M^{-1})	$[denaturant]_{1/2}$ (M)	concentration (μM)	$\Delta G°$ (kcal mol^{-1})	m (kcal mol^{-1} M^{-1})	$[denaturant]_{1/2}$ (M)
fluorescence[b]	10	4.7 ± 0.9	1.8 ± 0.3	2.60 ± 0.09	10	13 ± 1[f]	2.6 ± 0.4	2.53 ± 0.06
	20	5.9 ± 0.4	2.1 ± 0.2	2.71 ± 0.03	20	13 ± 1[f]	2.5 ± 0.4	2.64 ± 0.07
	20 (GdmCl)[c]	4.8 ± 0.6	4.3 ± 0.4	1.13 ± 0.02	30	11 ± 1[f]	2.1 ± 0.3	2.53 ± 0.08
					47	13 ± 1[f]	2.7 ± 0.2	2.84 ± 0.03
CD[d]	20	3.9 ± 0.8	1.5 ± 0.3	2.6 ± 0.1	20	8 ± 2	2.7 ± 0.9	2.9 ± 0.1
	30	3.4 ± 0.9	1.3 ± 0.4	2.6 ± 0.1	30	7 ± 2	2.5 ± 0.8	2.8 ± 0.1
	49	3.4 ± 0.9	1.3 ± 0.2	2.7 ± 0.1	55	4 ± 2	1.3 ± 0.9	2.9 ± 0.4

[a] $\Delta G°$ is the free energy of unfolding extrapolated to the absence of denaturant; m is the slope of the variation in the free energy of unfolding with denaturant concentration (urea or GdmCl). Errors in the m and $[denaturant]_{1/2}$ values are fitting errors. The uncertainty in $\Delta G°$ was obtained from error propagation, assuming that the errors in the m and $[denaturant]_{1/2}$ values are independent. Repetitions of the chemical denaturations yielded differences of 0.2 kcal mol^{-1} M^{-1} in the m values and 0.06 M in the $[denaturant]_{1/2}$ values. All experiments were performed at 25 °C and pH 7.0 in 10 mM Tris buffer. [b] All the fluorescence curves were obtained from the fluorescence intensity at 308 nm. [c] These measurements were taken in the presence of GdmCl. [d] The values were obtained by following the changes in the ellipticity at 222 nm. [e] The fluorescence curves were fitted to the equation corresponding to a bimolecular process (eq 6). The CD curves were fitted to the equation of a unimolecular transition, because no concentration dependence was observed (eq 4). [f] The free energy units are at a 1 M standard state.

spectra suggest that the protein was unfolded (Figure 4, left side), we favor that at low pH, the $RDTyrH_{65-159}$ was unfolded but we cannot rule out the presence of oligomeric species.

RDTyrH at pH 4.5 had an R_S of 77 ± 12 Å, with an estimated molecular weight of 80.9 kDa, suggesting that at low pH the protein strongly aggregated; the presence of this aggregated form could explain the smaller value of D obtained in the DOSY experiments [$(4.38 \pm 0.07) \times 10^{-7}$ cm^2 s^{-1}]. For an unfolded, monomeric 158-residue protein, the obtained R_S is 40 ± 18 Å, further suggesting that RDTyrH at this pH was not monomeric.

In summary, we can conclude that both RD species acquired a native-like tertiary structure and compactness near pH 7.0; however, secondary structure was acquired at acidic pHs. This earlier acquisition of secondary structure was not associated with the presence of the first 64 residues. However, we do not know whether the secondary structure is native-like.

The $RDTyrH_{65-159}$ Species Had a Smaller Conformational Stability. Because thermal denaturations were irreversible, we conducted urea denaturations to measure the conformational stability of both proteins by intrinsic fluorescence, CD, and SEC. In both proteins, urea denaturations were reversible (Figure 1 of the Supporting Information). We used urea as a denaturant because the fluorescence experiments with $RDTyrH_{65-159}$ in the presence of GdmCl yielded a short native baseline, thus causing a large slope (m value) in the denaturation curves of $RDTyrH_{65-159}$ (Table 3).

$RDTyrH_{65-159}$. Fluorescence and CD experiments at different protein concentrations had the same $[urea]_{1/2}$, showing the absence of the concentration dependence of this parameter; furthermore, $[urea]_{1/2}$ was the same via both techniques (Figure 6 of the Supporting Information). However, the m value (the slope of the transition) was slightly smaller in the CD experiments (and, thus, the transition was more cooperative) than in the fluorescence experiments (Table 3 and Figure 5A). The denaturation curves were fitted to the two-state model for a unimolecular transition. Urea denaturations followed by ANS fluorescence did not show any sigmoidal behavior (data not shown). In addition, the SEC experiments resulted in a slope-decreasing line as the urea concentration increased [Figure 5B (○)], but at 2.5 M urea, the peak eluted at elution volumes larger than the bed volume of the column, probably because of the interactions with the column. At urea concentrations larger than $[urea]_{1/2}$ (as determined by fluorescence and CD, ~2.5−2.8 M), the protein again started eluting at elution volumes smaller than the bed volume, although they were smaller than the volume at 0 M urea, due to the fact that the protein has a more expanded Stokes radius (as it is unfolded). These results suggest that $RDTyrH_{65-159}$ did not unfold through a two-state mechanism, despite its small size. We tried to fit the experimental data to a global (for all experiments in the two techniques) three-state process,[38] but we did not obtain a large improvement in the χ^2 of the fitting, when compared to that of the simplest two-state model.

RDTyrH. Fluorescence experiments showed a clear concentration dependence, and then as we did observe only a single sigmoidal transition (Figure 6A of the Supporting Information) (Table 2), we fitted the denaturation curves to a two-state bimolecular process (that is, dimer dissociation and unfolding of the resulting monomers occur concomitantly, in an all-or-none process) [eq 5 (see Experimental Procedures)].[28−30] On the other hand, the CD denaturation curves were concentration-independent (Figure 6B of the Supporting Information) (Table 2), showing similar m and $[urea]_{1/2}$ values. The exception was the denaturation curve obtained at the highest concentration (55 μM in protomer units), which had an m value slightly smaller than those at the lower protein concentrations (although they are similar within error); we think that the reason behind that smaller m value was the absence of enough data points at the unfolding baseline. Moreover, it can be observed that the CD denaturation curves at the higher concentrations (30 and 55 μM in protomer units) had a larger slope in the native baselines (Figure 6B of the Supporting Information), which could also affect the determination of the m value. As can be observed, either in fluorescence or in CD, the m values obtained for RDTyrH are larger than those measured for $RDTyrH_{65-159}$ (Table 3), suggesting that the denaturation curves of the larger species involved more than an unfolding step (see Discussion).

The free energies from fluorescence (and thus comprising dimer dissociation and monomer unfolding) of RDTyrH are in the range of 12 kcal mol^{-1}, similar to those measured in the dissociation and monomer unfolding of other dimeric proteins (Table 3 of ref 29). Conversely, the unimolecular process being monitored by CD has a free energy larger than that of the monomer $RDTyrH_{65-159}$ species (Table 3). Attempts to measure

DOI: 10.1021/acs.biochem.6b00135
Biochemistry 2016, 55, 3418−3431

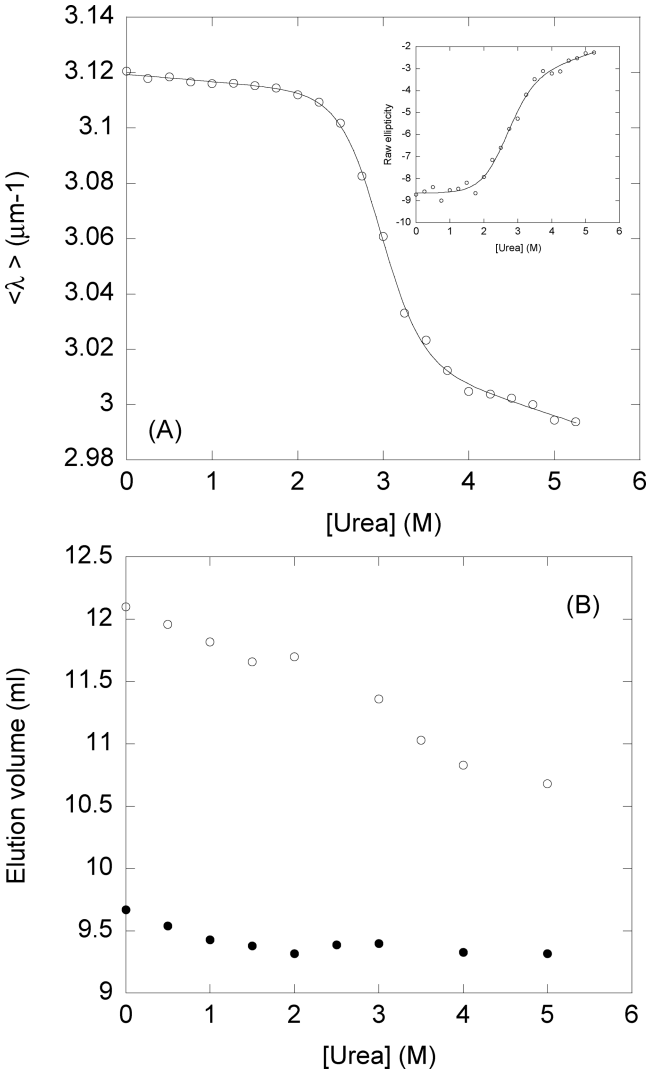

Figure 5. Chemical denaturation of $RDTyrH_{65-159}$. (A) $\langle\lambda\rangle$ from the intrinsic fluorescence of $RDTyrH_{65-159}$ at 10 μM protein (in protomer units). The inset shows the CD denaturation curve of $RDTyrH_{65-159}$ at 20 μM protein (in protomer units). (B) Gel filtration data for $RDTyrH_{65-159}$ (○) and RDTyrH (●). Protein concentrations in the gel filtration experiments were 150 μM (in protomer units), at all urea concentrations for both proteins. Experiments were conducted at 20 °C.

the compactness of the protein through gel filtration also failed since there was a decreasing line in the elution volumes as the urea concentration increased [Figure 5B (●)], because of the increase in the Stokes radius as the protein is unfolded [which happened in the $RDTyrH_{65-159}$ species (see above)]. The SEC results suggest that the dissociation-and-unfolding reaction of RDTyrH was not a two-state process.

DISCUSSION

pH Denaturation of RD Species. Only at pH ∼7.0 did the RD species acquire its native-like conformation, and it did so in two steps. First, it acquired secondary structure, and later, it acquired a native-like tertiary structure and compactness (as it buried all the solvent-exposed hydrophobic residues) (Figures 3 and 4). Thus, there are some pHs at which the protein has acquired secondary structure, but it has not attained a tertiary one; that is, it seems that both RD species populate at low pH a molten-globule-like species.[36] These results suggest that (i) compactness had a direct relationship with burial of solvent-exposed hydrophobic patches in RD species and (ii) the late acquisition of native-like compactness was not related to the presence of the disordered N-terminal residues, because both species showed a similar behavior. At low pH, where there is evidence of secondary structure, the RDTyrH seems to populate oligomeric molten-globule-like species, with noncooperative thermal transitions,[36,39] but we cannot unambiguously conclude that $RDTyrH_{65-159}$ populated also self-associated species (although the species populated by $RDTyrH_{65-159}$ showed molten-globule-like features, as well). These species (either oligomeric or not) in both RD proteins appear to be disordered from NMR results (Figure 4 and Figure 5 of the Supporting Information), but the CD experiments (Figure 3B) suggest unambiguously the presence of more helicity (higher ellipticity) than in the native state. These differences between both techniques (showing the CD spectra more ordered helix-like structure than the NMR ones) have been reported in highly flexible proteins.[40,41] At this stage, however, we do not know whether that secondary structure is native-like.

Because we know the structure of the dimeric RD species,[12] we can try to figure out which are (or is) the residues responsible for the acquisition of, first, secondary structure and, later, native-like tertiary structure and compactness by using Propka[42] (http://nbcr-222.ucsd.edu/pdb2pqr_2.0.0). However, it is important to keep in mind the predictive character of such calculations. From the predictions, the acquisition of secondary structure (occurring at a pK_a of 4.5 ± 0.2) is mainly associated with several acidic residues, namely, Asp141, Asp155, Glu70, Glu75, Glu76, Glu115, Glu130, and Glu136. On the other hand, the only predicted residue in the dimeric species with a pK_a (5.7) close to that obtained from fluorescence (intrinsic and ANS) measurements is His112 (close to the dimerization interface[12]). Conversely, in the monomer of RD species, the sole residue whose pK_a was close to the measured value (5.7) was Glu105. If $RDTyrH_{65-159}$ populated an oligomeric species at low pHs with a native-like quaternary arrangement, we could speculate that the residue implicated in the acquisition of secondary native-like structure was His112 (which is probably involved in such acquisition in RDTyrH, because it formed oligomeric species at low pH). However, because we do not have any unambiguous evidence of oligomeric species in the $RDTyrH_{65-159}$ at low pH, we suggest that Glu105 might be involved in the acquisition of the secondary structure.

Stability of the Monomeric Species of RDTyrH. The conformational free energy of monomeric RD species (evaluated as the average free energy change upon unfolding, ΔG, at 25 °C and pH 7.0) amounts to ∼4.7 kcal mol^{-1}, which is below those determined for most proteins (by 5−13 kcal mol^{-1}).[29,38,43−45] Because we know the structure of the dimeric species of $RDTyrH_{65-159}$, we can calculate the theoretically predicted value of the m slope from the chemical denaturation curves,[46] assuming that there was not any structural rearrangement upon dimerization (see below) and calculating the ASA of the monomer with VADAR.[47] We obtained values of 1.5 ± 0.3 kcal mol^{-1} M^{-1} (for the urea denaturations) and 3.0 ± 0.2 kcal mol^{-1} M^{-1} (for the GdmCl denaturations). Both theoretical values are smaller than those experimentally obtained (Table 1), suggesting that there are variations in the amount of ASA exposed upon unfolding with those predicted. However, it is important to indicate that such a value is within the range of those observed for monomeric species.[29,38] The experimental m values of the unimolecular denaturation far-UV CD curves of RDTyrH

DOI: 10.1021/acs.biochem.6b00135
Biochemistry 2016, 55, 3418−3431

were larger than those of the shorter species (Table 3). This higher value is within the range observed for some dimeric proteins[29,38] and, we think, is responsible for the greater conformational stability (7 kcal mol^{-1} vs 5 kcal mol^{-1}) (Table 3). Furthermore, this larger value of the free energy must be due to the presence of the 65 disordered N-terminal residues. If, we assume that (i) we can calculate the additional stabilization of the dimer by the ASA buried (770 Å^2 per monomer[12]) and (ii) we can apply the same equations to this surface[47] (interface), we find the m value for the dissociation ("unfolding" of the dimer) of this interface would be 2 × 0.4587 = 0.9174 kcal mol^{-1} M^{-1}. Then, this number should be added to the value of 1.5 kcal mol^{-1} M^{-1} previously obtained for the monomeric species of RDTyrH$_{65-159}$, which yields a value of 2.4 kcal mol^{-1} M^{-1}; this value is similar to the m value measured for dimeric RDTyrH (Table 3), even under the rough assumptions used. We suggest that although the far-UV CD was spectroscopically silent to dimer dissociation, it might report, through the variations in the m value, about such a bimolecular process.

The fact that CD does not report on dissociation is difficult to explain. The simplest explanation is to assume that upon dissociation both isolated monomers of RD species have the same structure as that when forming part of the dimer; that is, dissociation (or, alternatively, association to form the dimer) does not induce any large conformational rearrangement in any of the monomers, and therefore, association would be a perfect lock-and-key process. We observed in the CD denaturation curves at the higher explored concentrations of RDTyrH a large slope in the native baseline (Figure 6B of the Supporting Information). It could be argued that this slope is reporting on dissociation of the dimer (and that is why the longest slopes are observed only at the highest concentrations of protein, where the dimer is more populated); however, the findings that (i) the m values for the transitions at the highest concentrations are similar to that at the lower concentrations (Table 3) and (ii) these m values are consistent with a dimer dissociation and unfolding[29] suggest that the native baseline slope is associated with changes in the structure of the dimer, which do not involve dissociation.

Keeping in mind the limitations in calculation of the dissociation constant of RDTyrH (Figure 2C), we find the free energy of dissociation, obtained from the value of K_D [which accounts for $-RT \ln(K_D)$ = 7.8 kcal mol^{-1} (at a 1 M standard concentration)] plus the conformational free energy of the monomer [4.7 kcal mol^{-1} (Table 3)] is 12.5 kcal mol^{-1} (at 1 M standard state). This value is similar to that measured for the dissociation and unfolding of the dimeric species measured by fluorescence (Table 3), and then, we conclude that the tertiary interactions that may be established within each monomer only upon dimerization are very weak. That is, the structure of each isolated monomer of RD species is similar to that in the formed dimer, as hypothesized above, based on the absence of changes in CD upon dimer dissociation.

Self-Association of RD of TyrH. The solution structure of dimeric RDTyrH$_{65-159}$ has been determined recently by NMR.[12] In this work, we have shown that at the concentrations used (10−500 μM) the protein remained monomeric, as suggested by the several spectroscopic and biophysical techniques employed. Two factors can explain this apparent discrepancy. First, the triple-resonance experiments with double and triple labeled samples were conducted at concentrations of 800 μM; in most of the probes used in this work, we have explored until 500 μM (SEC experiments), but in the DLS experiments conducted at 800 μM, there was a slightly larger polydispersity of the peak, although the protein remained, at a large population, monomeric (Figure 2 of the Supporting Information). Second, to avoid possible degradation of samples during the long acquisition times of the NMR experiments, the highly concentrated protein samples contained 1 μM leupeptin and 1 μM pepstain; it has been suggested that addition of some compounds to concentrated protein solutions could stabilize the most oligomerized state of the protein.[48]

On the other hand, the same biophysical and spectroscopic techniques used in this work suggest that RDTyrH in the same range of concentrations is a dimer. We have explored theoretically the aggregation tendencies of both protein fragments by using Zygreggator,[49−51] and we have observed that the intrinsic aggregation propensity of RDTyrH is 1.5-fold larger than that of RDTyrH$_{65-159}$. Furthermore, we have been able to obtain the K_D of dimeric RDTyrH (1.6 μM) by zonal gel filtration chromatography. This value is smaller than that of RDPheH, which accounts for 46 ± 35 μM.[52] The RD domains of PheH and TyrH have similar structures, but they are not very similar in sequence; furthermore, the structure of the RD and catalytic regions of PheH does not show the presence of contacts between individual domains,[13] but RDTyrH was dimeric at the NMR concentrations.[12] Moreover, in RDPheH, the presence of the substrate (Phe) stabilizes the dimer,[52,53] but the presence of Tyr is not necessary to stabilize the dimer of RDTyrH. At this stage, we do not know, however, how the presence of the additional residues can modulate dimer formation, except for a stronger tendency of such an additional tail to aggregate. We do not know exactly the full implications of dimer formation in the functions of the RD, but we hypothesize that its unstable monomer could facilitate rapid switching off of signaling. We suggest that it is the higher affinity of dimeric RDTyrH that modulates the recognition of the substrate, thus modifying the mechanism of regulation of both proteins.[7,54] Further research must be conducted to determine how the dimerization of PheH affects its stability and whether the stability of its monomeric species is as low as that of RDTyrH.

■ ASSOCIATED CONTENT

Supporting Information

The Supporting Information is available free of charge on the ACS Publications website at DOI: 10.1021/acs.biochem.6b00135.

Urea refolding experiments for both species monitored by fluorescence (Figure 1), DLS experiments with RDTyrH$_{65-159}$ at two concentrations and two pHs (Figure 2), chromatograms obtained by analytical SEC for both species (Figure 3), ITC thermograms of both species at different concentrations (Figure 4), 1D ^{1}H NMR spectra of the RD species (Figure 5), chemical denaturation curves of RDTyrH followed by fluorescence and CD at different concentrations (Figure 6), and supplementary experimental procedures for DSC and DOSY measurements (PDF)

■ AUTHOR INFORMATION

Corresponding Author

*Instituto de Biología Molecular y Celular, Edificio Torregaitán, Universidad Miguel Hernández, Avda. del Ferrocarril s/n, 03202 Elche (Alicante), Spain. Telephone: +34 966658459. Fax: +34 966658758. E-mail: jlneira@umh.es.

DOI: 10.1021/acs.biochem.6b00135
Biochemistry 2016, 55, 3418−3431

Present Address

[‖]J.B.: Department of Chemistry and Biochemistry and Center for Applied Structural Discovery, The Biodesign Institute, Arizona State University, Tempe, AZ 85287-1604.

Funding

This work was supported by regional grants from Regional Generalitat Valenciana, Prometeo 018/2013 (J.L.N. and J.G.), Spanish Ministry of Economy and Competitiveness, and FEDER (EU) [BIO2012-39922-C02-01/02 (A.C.-A.) and CTQ2015-64445-R (J.L.N. and J.G.)]. F.H. was supported by Prometeo 018/2013.

Notes

The authors declare no competing financial interest.

■ ACKNOWLEDGMENTS

We thank two reviewers for helpful comments and experimental suggestions. We deeply thank May García, María del Carmen Fuster, and Javier Casanova for excellent technical assistance. We thank Prof. Paul F. Fitzpatrick for the kind gift of the RDTyrH and RDTyrH$_{65-159}$ vectors. We thank Dr. Shengnan Zhang and Prof. Paul F. Fitzpatrick for helpful suggestions and ideas about purification of both proteins and for reading early versions of the manuscript.

■ ABBREVIATIONS

ANS, 8-anilinonaphthalene-1-sulfonic acid; ASA, accessible surface area; CD, circular dichroism; DOSY, diffusion ordered spectroscopy; DLS, dynamic light scattering; DSC, differential scanning calorimetry; *D*, translational self-diffusion coefficient; GdmCl, guanidine hydrochloride; ITC, isothermal titration calorimetry; NMR, nuclear magnetic resonance; PheH, phenylalanine hydroxylase; RD, regulatory domain; RDPheH, regulatory domain of phenylalanine hydroxylase; RDTyrH, regulatory domain of tyrosine hydroxylase, containing residues 1−159 of the whole RD; RDTyrH$_{65-159}$, region of the RD of TyrH containing the well-folded core of the protein; R_S, hydrodynamic radius; SEC, size exclusion chromatography; TSP, 3-(trimethylsilyl)propionic acid-2,2,3,3-$^2H_4$-sodium salt; TyrH, tyrosine hydroxylase; UV, ultraviolet.

■ REFERENCES

(1) Nagatsu, T., Levitt, M., and Underfriend, S. (1964) Tyrosine hydroxylase: the initial step in norepinephrine biosysnthesis. *J. Biol. Chem. 239*, 2910−2917.

(2) Zigmond, R. E., Schwarzschild, M. A., and Rittenhouse, A. R. (1989) Acute regulation of tyrosine hydroxylase by nerve activity and by neurotransmitters *via* phosphorylation. *Annu. Rev. Neurosci. 12*, 415−461.

(3) Ishiguro, H., Arinami, T., Saito, T., Akazawa, S., Enomoto, M., Mitushio, H., Fujishiro, H., Tada, K., Akimoto, Y., Mifune, H., Shiozuka, S., Hamaguchi, H., Toru, M., and Shibuya, H. (1998) Systematic search for variations in the tyrosine hydroxylase gene and their associations with schizophrenia, affective disorders, and alcoholism. *Am. J. Med. Genet. 81*, 388−396.

(4) Kunugi, H., Kawada, Y., Hattori, M., Ueki, A., Otsuka, M., and Nanko, S. (1998) Association study of structural mutations of the tyrosine hydroxylase gene with schizophrenia and Parkinson's disease. *Am. J. Med. Genet. 81*, 131−133.

(5) Hoffmann, G. F., Assmann, B., Bräutigam, C., Dionisi-Vici, C., Häussler, M., de Klerk, J. B., Naumann, M., Steenbergen-Spanjers, G. C., Strassburg, H. M., and Wevers, R. A. (2003) Tyrosine hydroxylase deficiency causes progressive encephalopathy and dopa-nonresponsive distonia. *Ann. Neurol. 54*, S56−65.

(6) Rao, F., Zhang, K., Zhang, L., Rana, B. K., Wessel, J., Fung, M. M., Rodríguez-Flores, J. L., Taupenot, L., Ziegler, M. G., and O'Connor, D. T. (2010) Human tyrosine hydroxylase natural allelic variation: influence on autonomic function and hypertension. *Cell. Mol. Neurobiol. 30*, 1391−1394.

(7) Fitzpatrick, P. F. (1999) Tetrahydropterin-dependent amino acid hydroxylases. *Annu. Rev. Biochem. 68*, 355−381.

(8) Grima, B., Lamouroux, A., Blanot, F., Biguet, N. F., and Mallet, J. (1985) Complete coding sequence of rat tyrosine hydroxylase mRNA. *Proc. Natl. Acad. Sci. U. S. A. 82*, 617−621.

(9) Goodwill, K. E., Sabatier, C., Marks, C., Raag, R., Fitzpatrick, P. F., and Stevens, R. C. (1997) Crystal structure of tyrosine hydroxylase at 2.3 Å and its implications for inherited neurodegenerative diseases. *Nat. Struct. Biol. 4*, 578−585.

(10) Lohse, D. L., and Fitzpatrick, P. F. (1993) Identification of the intersubunit binding region in rat tyrosine hydroxylase. *Biochem. Biophys. Res. Commun. 197*, 1543−1548.

(11) Daubner, S. C., Lohse, D. L., and Fitzpatrick, P. F. (1993) Expression and characterization of catalytic and regulatory domains of rat tyrosine hydroxylase. *Protein Sci. 2*, 1452−1460.

(12) Zhang, S., Huang, T., Ilangovan, U., Hinck, A. P., and Fitzpatrick, P. F. (2014) The solution structure of the regulatory domain of tryrosine hydroxylase. *J. Mol. Biol. 426*, 1483−1497.

(13) Kobe, B., Jennings, I. G., House, C. M., Michell, B. J., Goodwill, K. E., Santarsiero, B. D., Stevens, R. C., Cotton, R. G. H., and Kemp, B. E. (1999) Structural basis of autoregulation of phenylalanine hydroxylase. *Nat. Struct. Biol. 6*, 442−448.

(14) Grant, G. A. (2006) The ACT domain: a small molecule binding domain and its role as a common regulatory element. *J. Biol. Chem. 281*, 33825−33829.

(15) Pace, C. N., and Scholtz, J. M. (1997) Measuring the conformational stability of a protein. In *Protein Structure* (Creighton, T. E., Ed.) 2nd ed., pp 253−259, Oxford University Press, Oxford, U.K.

(16) Piotto, M., Saudek, V., and Sklenar, V. (1992) Gradient-tailored excitation for single-quantum NMR spectroscopy of aqueous solutions. *J. Biomol. NMR 2*, 661−665.

(17) Czypionka, A., Ruiz de los Paños, O., Mateu, M. G., Barrera, F. N., Hurtado-Gómez, E., Gómez, J., Vidal, M., and Neira, J. L. (2007) The isolated C-terminal domain of Ring 1B is a dimer made of stable, well-structured monomers. *Biochemistry 46*, 12764−12776.

(18) Wilkins, D. K., Grimshaw, S. B., Receveur, V., Dobson, C. M., Jones, J. A., and Smith, L. J. (1999) Hydrodynamic radii of native and denatured proteins measured by pulse field gradient NMR techniques. *Biochemistry 38*, 16424−16431.

(19) Darling, P. J., Holt, J. M., and Ackers, G. K. (2000) Coupled energetics of lambda cro repressor self-assembly and site-specific DNA operator binding I: analysis of cro dimerization from nanomolar to micromolar concentrations. *Biochemistry 39*, 11500−11507.

(20) Muro-Pastor, M. I., Barrera, F. N., Reyes, J. C., Florencio, F. J., and Neira, J. L. (2003) The inactivating factor of glutamine synthetase, IF7, is a "natively unfolded" protein. *Protein Sci. 12*, 1443−1454.

(21) Ackers, G. K. (1967) Molecular sieve studies of interacting protein systems. I. Equations for transport of associating systems. *J. Biol. Chem. 242*, 3026−3034.

(22) Hinkle, A., Goranson, A., Butters, C. A., and Tobacman, L. S. (1999) Roles for the troponin tail domain in thin filament assembly and regulation. A deletional study of cardiac troponin T. *J. Biol. Chem. 274*, 7157−7164.

(23) Spiegel, M. R. (1985) *Probability and statistics*, McGraw Hill, New York.

(24) Neira, J. L., Román-Trufero, M., Contreras, L. M., Prieto, J., Singh, G., Barrera, F. N., Renart, M. L., and Vidal, M. (2009) The transcriptional repressor RYBP is a natively unfolded protein which folds upon binding to DNA. *Biochemistry 48*, 1348−1360.

(25) Royer, C. A. (1995) in *Protein stability and folding* (Shirley, B. A., Ed.) pp 65−89, Humana Press, Towota, NJ.

(26) Lakowicz, J. R. (1999) *Principles of fluorescence spectroscopy*, 2nd ed., Plenum Press, New York.

DOI: 10.1021/acs.biochem.6b00135
Biochemistry 2016, 55, 3418−3431

(27) Benjwal, S., Verma, S., Röhm, K. H., and Gursky, O. (2006) Monitoring protein aggregation during thermal unfolding in circular dichroism experiments. *Protein Sci. 15*, 635−639.
(28) Mateu, M. G. (2002) Conformational stability of dimeric and monomeric forms of the C-terminal domain of human immnunodeficiency virus-1 capsid protein. *J. Mol. Biol. 318*, 519−531.
(29) Rumfeldt, J. A.O., Galvagnion, C., Vassall, K. A., and Meiering, E. M. (2008) Conformational stability and folding mechanisms of dimeric proteins. *Prog. Biophys. Mol. Biol. 98*, 61−84.
(30) Bedouelle, H. (2016) Principles and equations for measuring an interpreting protein stability: from monomer to tetramer. *Biochimie 121*, 29−37.
(31) Cantor, C. R., and Schimmel, P. R. (1980) *Biophysical Chemistry*, W. H. Freeman, New York.
(32) Creighton, T. E. (1993) *Proteins. Structures and macromolecular properties*, 2nd ed., W. H. Freeman, New York.
(33) Cavanagh, J. F., Wayne, J., Palmer, A. G., III, and Skelton, N. J. (1996) *Protein NMR spectroscopy: Principles and practice*, Academic Press, San Diego.
(34) Yao, S., Babon, J. J., and Norton, R. S. (2008) Protein effective correlation times from translational self-diffusion coefficients measured by PFG-NMR. *Biophys. Chem. 136*, 145−151.
(35) Daragan, V. A., and Mayo, K. H. (1997) Motional model analyses of protein and peptide dynamics using ^{13}C and ^{15}N NMR relaxation. *Prog. Nucl. Magn. Reson. Spectrosc. 31*, 63−105.
(36) Ptitsyn, O. B. (1995) Molten globule and protein folding. *Adv. Protein Chem. 47*, 83−229.
(37) Wüthrich, K. (1986) *NMR of proteins and nucleic acids*, John Wiley & Sons, New York.
(38) Sancho, J. (2013) The stability of 2-state, 3-state and more-state proteins from simple spectroscopic techniques··· plus the structure of the equilibrium intermediates at the same time. *Arch. Biochem. Biophys. 531*, 4−13.
(39) Fink, A. L. (1995) Compact intermediate states in protein folding. *Annu. Rev. Biophys. Biomol. Struct. 24*, 495−522.
(40) Alcaraz, L. A., del Álamo, M., Mateu, M. G., and Neira, J. L. (2008) Structural mobility of the C-terminal domain of the HIV-1 capsid protein. *FEBS J. 275*, 3299−3311.
(41) Mayor, U., Guydosh, N. R., Johnson, C. M., Grossmann, G., Sato, S., Jas, G. S., Freund, S. M. V., Alonso, D. O. V., Daggett, V., and Fersht, A. R. (2003) The complete folding pathway of a protein from nanosecond to microsecond. *Nature 421*, 863−867.
(42) Li, H., Robertson, A. D., and Jensen, J. H. (2005) Very fast empirical prediction and rationalization of protein pK_a values. *Proteins: Struct., Funct., Genet. 61*, 704−721.
(43) Neet, K. E., and Timm, D. E. (1994) Conformational stability of dimeric proteins: quantitative studies by equilibrium denaturation. *Protein Sci. 3*, 2167−2174.
(44) Doyle, C. M., Rumfeldt, J. E., Broom, H. R., Broom, A., Stathopulos, B., Vassall, K. A., Almey, J. J., and Meiering, E. M. (2013) Energetics of oligomeric protein folding and association. *Arch. Biochem. Biophys. 531*, 44−64.
(45) Freire, E. (2003) in *Protein Structure, Stability, and Folding* (Murphy, K. P., Ed.) pp 37−68, Humana Press, Totowa, NJ.
(46) Myers, J. K., Pace, C. N., and Scholtz, J. M. (1995) Denaturant m values and heat capacity changes: Relation to changes in accessible surface areas of protein unfolding. *Protein Sci. 4*, 2138−2148.
(47) Willard, L., Ranjan, A., Zhang, H., Monzavi, H., Boyko, R. F., Sykes, B. D., and Wishart, D. S. (2003) VADAR: A web server for quantitative evaluation of protein structure quality. *Nucl. Acid. Res. 31*, 3316−3319.
(48) Macchi, F., Eisenkolb, M., Kiefer, H., and Otzen, D. E. (2012) The effects of osmolytes on protein fibrillation. *Int. J. Mol. Sci. 13*, 3801−3819.
(49) DuBay, K. F., Pawar, A. P., Chiti, F., Zurdo, J., Dobson, C. M., and Vendruscolo, M. (2004) Prediction of the absolute aggregation rates of amyloidogenic polypeptide chains. *J. Mol. Biol. 341*, 1317−1326.
(50) Pawar, A. P., DuBay, K. F., Zurdo, J., Chiti, F., Vendruscolo, M., and Dobson, C. M. (2005) Prediction of "aggregation-prone" and "aggregation-susceptible" regions in proteins associated with neurodegenerative diseases. *J. Mol. Biol. 350*, 379−392.
(51) Tartaglia, G. G., Pawar, A. P., Campioni, S., Chiti, F., Dobson, C. M., and Vendruscolo, M. (2008) Prediction of aggregation-prone of structure proteins. *J. Mol. Biol. 380*, 425−436.
(52) Zhang, S., Roberts, K. M., and Fitzpatrick, P. F. (2014) Phneylalanine binding is linked to dimerization of the regulatory domain of phenylalanine hydroxylase. *Biochemistry 53*, 6625−6627.
(53) Zhang, S., Hinck, A. P., and Fitzpatrick, P. F. (2015) The amino acid specificity for activation of phenylalanine hydroxylase matches the specificity for stabilization of regulatory domain dimers. *Biochemistry 54*, 5167−5174.
(54) Daubner, S. C., Le, T., and Wang, S. (2011) Tyrosine hydroxylase and regulation of dopamine synthesis. *Arch. Biochem. Biophys. 508*, 1−12.
(55) DeLano, W. L. (2002) *The PyMOL molecular graphics system*, DeLano Scientific, Palo Alto, CA.

DOI: 10.1021/acs.biochem.6b00135
Biochemistry 2016, 55, 3418−3431